

# Local radiative feedback in the formation of the first protogalaxies

Jarrett L. Johnson<sup>1</sup>, Thomas H. Greif<sup>1,2,3</sup>, and Volker Bromm<sup>1</sup>

## ABSTRACT

The formation of the first galaxies is influenced by the radiative feedback from the first generations of stars. This feedback is manifested by the heating and ionization of the gas which lies within the H II regions surrounding the first stars, as well as by the photodissociation of hydrogen molecules within the larger Lyman-Werner (LW) bubbles that surround these sources. Using a ray-tracing method in three-dimensional cosmological simulations, we self-consistently track the formation of, and radiative feedback from, individual stars in the course of the formation of a protogalaxy. We compute in detail the H II regions of each of these sources, as well as the regions affected by their molecule-dissociating radiation. We follow the thermal, chemical, and dynamical evolution of the primordial gas as it becomes incorporated into the protogalaxy. While the IGM is, in general, optically thick to LW photons only over physical distances of  $\gtrsim 30$  kpc at redshifts  $z \lesssim 20$ , the high molecule fraction that is built up in relic H II regions and their increasing volume-filling factor renders even the local IGM optically thick to LW photons over physical distances of the order of a few kiloparsecs. We find that efficient accretion onto Pop III relic black holes may occur after  $\sim 60$  Myr from the time of their formation, by which time the photo-heated relic H II region gas can cool and re-collapse into the  $10^6 M_{\odot}$  minihalo which hosts the black hole. Also, Pop II.5 stars, postulated to have masses of the order of  $10 M_{\odot}$ , can likely form from this re-collapsing relic H II region gas, but their formation may be suppressed by LW feedback from neighboring star-forming regions. Overall, we find that the local radiative feedback from the first generations of stars suppresses the star formation rate by only a factor of, at most, a few.

*Subject headings:* stars: formation — molecular processes — H II regions — galaxies: formation — early universe — cosmology: theory

---

<sup>1</sup>Department of Astronomy, University of Texas at Austin, 2511 Speedway, Austin, TX 78712; jljohnson@astro.as.utexas.edu, vbromm@astro.as.utexas.edu

<sup>2</sup>Institut für Theoretische Astrophysik, Universität Heidelberg, Albert-Ueberle-Strasse 2, 69120 Heidelberg, Germany; tgreif@ita.uni-heidelberg.de

<sup>3</sup>Fellow of the International Max Planck Research School for Astronomy and Cosmic Physics at the University of Heidelberg

## 1. Introduction

The formation of the earliest galaxies plays a key role in a number of the most important questions being addressed in cosmology today. The first galaxies are predicted to have been the dominant sources of the radiation which reionized the universe (e.g. Ciardi et al. 2006), and they may have hosted the majority of primordial star formation (Greif & Bromm 2006; but see also Jimenez & Haiman 2006). They are the likely sites for the formation of the most metal-poor stars that have recently been found in our Galaxy (e.g. Christlieb et al. 2002; Beers & Christlieb 2005; Frebel et al. 2005), and possibly for the first efficient accretion onto the stellar black holes (see Johnson & Bromm 2007) which may have been the seeds for the  $\sim 10^9 M_\odot$  black holes that are inferred at redshifts  $z \gtrsim 6$  (Fan et al. 2004, 2006). Furthermore, an understanding of the formation of the first galaxies is crucial for the interpretation of galaxies now beginning to be observed at  $z \gtrsim 6$  (e.g. Mobasher et al. 2005; Iye et al. 2006; Bouwens & Illingworth 2006), as well as of the objects at redshifts  $z \gtrsim 10$  which are expected to be detected with upcoming telescopes such as the *James Webb Space Telescope (JWST)* (Gardner et al. 2006). Among these systems there promise to be some of the first metal-free objects that will be observable, and as such it is important that theoretical predictions of their properties are made.

What were the effects of the radiative feedback from the first generations of stars on the formation of the first galaxies? It is now widely held that the first stars (termed Population III) were likely very massive, and therefore emitted copious amounts of radiation which profoundly affected their surroundings (Bromm et al. 1999, 2002; Abel et al. 2002; Yoshida et al. 2006; Gao et al. 2007). Recent work has demonstrated that the H II regions surrounding the first stars were able to evacuate the primordial gas from the minihalos that hosted these objects (Whalen et al. 2004; Kitayama et al. 2004; Alvarez et al. 2006; Abel et al. 2006). The impact of these H II regions on second generation star formation is complex (e.g. Ricotti, Gnedin & Shull 2001; Oh & Haiman 2003; Ahn & Shapiro 2006; Susa & Umemura 2006). While initially the density in these regions is suppressed and the gas within heated to  $\gtrsim 10^4$  K, vigorous molecule formation can take place once the gas begins to cool and recombine after the central Pop III star has collapsed to form a massive black hole, leading to the possibility of the formation of low-mass primordial stars (Nagakura & Omukai 2005; O’Shea et al. 2005; Johnson & Bromm 2006, 2007; Yoshida et al. 2007).

An additional radiative feedback effect from the first stars is the photo-dissociation of the fragile hydrogen molecules which allow the primordial gas to cool and collapse into minihalos, with virial temperatures  $\lesssim 8,000$  K (e.g. Barkana & Loeb 2001). The effects of the molecule-dissociating radiation from the first stars can reach far beyond their H II regions (e.g. Ciardi et al. 2000), and thus star formation in distant minihalos may have

been delayed or quenched altogether (e.g. Haiman et al. 1997, 2000; Mackey et al. 2003). Interestingly, however, while the general intergalactic medium (IGM) at the epoch of the first stars becomes optically thick to Lyman-Werner (LW) photons only over vast distances (e.g. Haiman et al. 2000; see also Glover & Brand 2001), the high molecule fraction that persists inside the first relic H II regions leads to a high optical depth to these photons, potentially allowing star formation to take place in minihalos down to lower redshifts than would otherwise be possible (Ricotti et al. 2001; Oh & Haiman 2002; Machacek et al. 2001, 2003; Johnson & Bromm 2007).

In the present work, we self-consistently track the formation of, and the radiative feedback from, individual Pop III stars in the course of the formation of a primordial protogalaxy. We compute in detail the H II regions and LW bubbles of each of these sources, and follow the evolution of the primordial gas as it becomes incorporated into the protogalaxy. In § 2, we describe our numerical methodology. Our results are presented in § 3, while we summarize our conclusions and discuss their implications in § 4.

## 2. Methodology

### 2.1. Cosmological Initial Conditions and Resolution

We employ the parallel version of GADGET for our three-dimensional numerical simulations. This code includes a tree, hierarchical gravity solver combined with the smoothed particle hydrodynamics (SPH) method for tracking the evolution of the gas (Springel, Yoshida & White 2001). Along with  $\text{H}_2$ ,  $\text{H}_2^+$ ,  $\text{H}$ ,  $\text{H}^-$ ,  $\text{H}^+$ ,  $\text{e}^-$ ,  $\text{He}$ ,  $\text{He}^+$ , and  $\text{He}^{++}$ , we have included the five deuterium species  $\text{D}$ ,  $\text{D}^+$ ,  $\text{D}^-$ ,  $\text{HD}$  and  $\text{HD}^-$ , using the same chemical network as in Johnson & Bromm (2006, 2007).

We carry out a three-dimensional cosmological simulation of high- $z$  structure formation which evolves both the dark matter and baryonic components, initialized according to the  $\Lambda$ CDM model at  $z = 100$ . As in earlier work (Bromm et al. 2003; Johnson & Bromm 2007), we adopt the cosmological parameters  $\Omega_m = 1 - \Omega_\Lambda = 0.3$ ,  $\Omega_B = 0.045$ ,  $h = 0.7$ , and  $\sigma_8 = 0.9$ , close to the values measured by *WMAP* in its first year (Spergel et al. 2003). Here we use a periodic box with a comoving size  $L = 460 h^{-1}$  kpc, but unless stated explicitly, we will always refer to physical distances in the present work. Our simulation uses a number of particles  $N_{\text{DM}} = N_{\text{SPH}} = 128^3$ , where the SPH particle mass is  $m_{\text{SPH}} \sim 740 M_\odot$ .

We have determined the maximum density of gas that can be reliably resolved in this simulation by carrying out a cosmological simulation from  $z = 100$ , in which we allow the gas to cool and collapse into minihalos without including radiative effects. We then compare

the minimum resolved mass, which we take to be  $\sim 64 m_{\text{SPH}}$ , with the Bonnor-Ebert mass, given by (see, e.g., Palla 2002)

$$M_{\text{BE}} \simeq 700 M_{\odot} \left( \frac{T}{200 \text{ K}} \right)^{3/2} \left( \frac{n}{10^4 \text{ cm}^{-3}} \right)^{-1/2}, \quad (1)$$

where  $n$  and  $T$  are the number density and temperature of the gas, respectively. As shown in Figure 1, the gas evolves according to the canonical behavior of primordial gas collapsing in minihalos (see, e.g., Bromm et al. 2002). We expect the gas in our simulations with radiative feedback to behave similarly as it collapses to high densities, since it is the formation of, and cooling by, molecules which will drive the collapse in both cases. Thus, we take the maximum density that we can reliably resolve to be that at which the Bonnor-Ebert mass becomes equal to the resolution mass. As is evident in Figure 1, this criterion results in a maximum resolvable density of  $n_{\text{res}} \sim 20 \text{ cm}^{-3}$ . This density is four orders of magnitude higher than the background mean density at a redshift of  $z \gtrsim 15$ , and such overdensities only occur in the minihalos within which the first Pop III stars form (see, e.g., Bromm & Larson 2004; Yoshida et al. 2006). We take it here that one Pop III star, assumed to have a mass of  $100 M_{\odot}$ , will form from this dense, collapsing primordial gas inside a minihalo, consistent with recent work which shows that, in general, only single stars are expected to form in minihalos under these conditions (Yoshida et al. 2006). Pop III stars with this mass are predicted to directly collapse to a black hole, and therefore produce no supernova explosion (e.g. Heger et al. 2003), which allows us to self-consistently neglect the possibility of ejection of metals into the primordial gas. We will consider this possibility in future work. In the present work, we focus on the radiative feedback from the first stars.

## 2.2. Radiative Feedback

In our simulations with radiative feedback, we assume that stars are formed in minihalos which acquire densities higher than  $n_{\text{res}} = 20 \text{ cm}^{-3}$ . In order to account for the radiative feedback from a star formed in a minihalo, the gas surrounding the star is first photo-heated. We then calculate the extent of the H II region, as well as of the LW bubble around the star. We carry out this procedure every time a star forms in the simulation. The Pop III star will soon die, and we then let the simulation evolve once more, allowing recombination to take place in the relic H II region, and for molecules to reform within the relic LW bubble. We expect that this procedure will provide reliable results, as the  $\lesssim 3 \text{ Myr}$  lifetime of a Pop III star is short compared to the typical dynamical times of the gas in this simulation.

### 2.2.1. Photoionization

To account for the presence of a  $100 M_{\odot}$  Pop III star in the minihalos in which the gas collapses to a density of  $n_{\text{res}}$ , we first photoheat and photoionize the gas within 500 pc of the gas particle which first reaches this density for a duration of the lifetime of the star, using the same heating and ionization rates as in Johnson & Bromm (2007). Our choice of a 500 pc radius ensures that the entire gas within the source minihalo, with virial radius  $\sim 150$  pc, is photoheated, but that we do not photoheat the dense, neutral gas in neighboring halos. Just as in this previous work, we reproduce the basic density and velocity structure of the gas within 500 pc of the central source that has been found in detailed one-dimensional radiation hydrodynamics calculations (Kitayama et al. 2004; Whalen et al. 2004).

Once this density structure is in place around the point source, we employ a ray-tracing technique to solve for the H II region that surrounds the star at the end of its life. We cast rays in  $N_{\text{ray}} \sim 100,000$  directions from the central source, and divide each ray into 500 segments. Then, we add up all of the recombinations that take place over the course of the star’s lifetime in each bin along each of the  $N_{\text{ray}}$  rays, taking the number of recombinations to be

$$N_{\text{rec}} = \alpha_{\text{B}} n_{\text{mean}}^2 \frac{4\pi}{N_{\text{ray}}} t_* r^2 dr , \quad (2)$$

where  $\alpha_{\text{B}}$  is the case B recombination coefficient,  $r$  is the distance of the bin from the star,  $dr$  is length of the bin in the direction radial to the star, and  $t_*$  is the lifetime of the star, here taken to be 3 Myr (Schaerer 2002). We compute  $n_{\text{mean}}$ , the average number density of hydrogen atoms in a bin, as

$$n_{\text{mean}} = \frac{\sum n_{\text{H}}}{N_{\text{part}}} . \quad (3)$$

Here  $N_{\text{part}}$  is the number of SPH particles in the bin and  $n_{\text{H}}$  is the number density of hydrogen of the individual SPH particles in that bin.

Next, we assume that the star radiates an equal number of photons in every direction, and we take the total number of ionizing photons that it radiates in its lifetime to be

$$N_{\text{ion}} = Q_{\text{ion}} t_* , \quad (4)$$

where we have chosen  $Q_{\text{ion}}$ , the average number of ionizing photons emitted per second by the star, to be  $10^{50} \text{ s}^{-1}$  (see Bromm et al. 2001; Schaerer 2002). We then add up the recombinations in all of the bins, along each of the rays, beginning with those closest to the

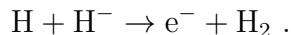
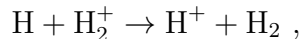
star and moving outward, until the number of recombinations along a ray equals the number of ionizing photons that are emitted along that ray. If the number of recombinations in the bin falls below the number of atoms in the bin, then we count the number of atoms in the bin against the number of photons as well. Doing this for each of the rays, we solve in detail for the H II region of the star. We set the free electron fraction to unity for each of the SPH particles that lie within the H II region. We set the temperature of the SPH particles within the H II region, but outside of the 500 pc photo-heated region, to  $T = 18,000$  K, roughly the value at the outer edge of the photo-heated region. As well, the fraction of molecules in the H II region is set to zero, as we assume that all molecules are collisionally dissociated at the high temperatures in the H II region.

### 2.2.2. Photodissociation

To find the region in which the LW radiation from the star destroys  $\text{H}_2$  and HD molecules, the “LW bubble” in our terminology, we carry out a ray-tracing procedure similar to the one used to solve for the H II region. We use the same bins as in that procedure, but now we evaluate the formation time of  $\text{H}_2$  molecules in each bin and compare this both to the lifetime of the star and to the dissociation time of the molecules. For each bin, we compute the  $\text{H}_2$  formation time as

$$t_{\text{form,H}_2} = \sum \frac{n_{\text{H}_2}}{n_{\text{H}}(k_1 n_{\text{H}_2^+} + k_2 n_{\text{H}^-})} / N_{\text{part}} , \quad (5)$$

where  $n_{\text{H}_2^+}$  and  $n_{\text{H}^-}$  are the number densities of  $\text{H}_2^+$  and  $\text{H}^-$ , respectively. The sum is over all the particles in the bin,  $N_{\text{part}}$ , and  $k_1$  and  $k_2$  are the rate coefficients for the following two main reactions that produce  $\text{H}_2$ :



We adopt the following values for these rate coefficients (de Jong 1972; Karpas et al. 1979; Haiman et al. 1996):

$$k_1 = 6.4 \times 10^{-10} \text{cm}^3 \text{s}^{-1} , \quad (6)$$

$$k_2 = 1.3 \times 10^{-9} \text{cm}^3 \text{s}^{-1} . \quad (7)$$

The dissociation time for the molecules is obtained by finding the flux of LW photons from a  $100 M_{\odot}$  Pop III star, assumed to be a blackbody emitter with radius  $R_* \simeq 3.9R_{\odot}$  and effective temperature  $T_* \simeq 10^5$  K (e.g., Bromm et al. 2001). The dissociation time for unshielded molecules at a distance  $R$  from the star is then given by (Abel et al. 1997)

$$t_{\text{diss,H}_2} \sim 10^5 \text{ yr} \left( \frac{R}{1 \text{ kpc}} \right)^2 . \quad (8)$$

Next, we note that for molecules to be effectively dissociated by the LW radiation, the dissociation time of the molecules must be shorter than both the lifetime of the star and the formation time of the molecules. Therefore, we compare all of these timescales for each bin along each ray and set the fraction of molecules to zero if  $t_{\text{diss,H}_2} \lesssim t_{\text{form,H}_2}$  and  $t_{\text{diss,H}_2} \lesssim t_*$ . If this condition is not satisfied, then the molecule fraction is left unchanged from its value before the formation of the star. This allows for the possibility of the effective shielding of  $\text{H}_2$  molecules because it accounts for the build-up of  $\text{H}_2$  column density, for instance, in relic H II regions or in collapsing minihalos where the formation time of  $\text{H}_2$  is relatively short.

We take into account the effects of self-shielding by adding up the  $\text{H}_2$  column density  $N(\text{H}_2)$  along the ray contributed by each bin in which the molecules are not effectively dissociated. We then adjust the dissociation time for the molecules in shielded bins according to (Draine & Bertoldi 1996):

$$t_{\text{diss,H}_2} \sim 10^5 \text{ yr} \left( \frac{R}{1 \text{ kpc}} \right)^2 \left( \frac{N(\text{H}_2)}{10^{14} \text{ cm}^{-2}} \right)^{0.75} , \quad (9)$$

when the column density of molecules between the bin and the star is  $N(\text{H}_2) \gtrsim 10^{14} \text{ cm}^{-2}$ .

The ionic species  $\text{H}^-$  and  $\text{H}_2^+$ , which are reactants in the main reactions which form  $\text{H}_2$ , can also, in principle, be destroyed by the radiation from the star. The photo-dissociation times for these species are given in terms of the temperature of the star  $T_*$ , the source of thermal radiation in our case, and the distance from the star  $R$ , as (Dunn 1968; de Jong 1972; Galli & Palla 1998)

$$t_{\text{diss,H}_2^+} = 5 \times 10^{-2} T_*^{-1.59} \exp\left(\frac{82000}{T_*}\right) \left(\frac{R}{R_*}\right)^2 \text{ s} , \quad (10)$$

$$t_{\text{diss,H}^-} = 9.1 T_*^{-2.13} \exp\left(\frac{8823}{T_*}\right) \left(\frac{R}{R_*}\right)^2 \text{ s} . \quad (11)$$

For the  $100M_{\odot}$  star, we find that  $t_{\text{diss},\text{H}_2^+} \sim 5 \times 10^3 \text{ yr } (\frac{R}{1\text{kpc}})^2$  and  $t_{\text{diss},\text{H}^-} \sim 9 \times 10^2 \text{ yr } (\frac{R}{1\text{kpc}})^2$ . The formation times for these species, on the other hand, are

$$t_{\text{form},\text{H}^-} = n_{\text{H}^-} \left( \frac{dn_{\text{H}^-}}{dt} \right)^{-1} \sim 3 \times 10^3 \text{ yr} , \quad (12)$$

$$t_{\text{form},\text{H}_2^+} = n_{\text{H}_2^+} \left( \frac{dn_{\text{H}_2^+}}{dt} \right)^{-1} \sim 4 \times 10^3 \text{ yr} , \quad (13)$$

for primordial gas at a temperature of  $T = 100 \text{ K}$  and a density of  $n_{\text{H}} = 10^{-2} \text{ cm}^{-3}$ , typical for gas at the outskirts of a collapsing minihalo. These formation timescales become much shorter for gas deeper inside minihalos, where the densities and temperatures are generally higher. It is in these regions, in and around minihalos, where the presence of molecules is most important for cooling the gas. Within these regions the photo-dissociation times for these ionic species are less than their formation times only if they are located  $\lesssim 2 \text{ kpc}$  from the star. Thus, photo-dissociation of these species will become ineffective at distances  $\gtrsim 2 \text{ kpc}$  from the star, a distance comparable to the size of the H II region of a Pop III star (Alvarez et al. 2006; Abel et al. 2006). Since we assume that molecules are collisionally destroyed inside the H II region, and since the LW bubble will generally be larger than the H II region, we ignore the photo-dissociation of  $\text{H}^-$  and  $\text{H}_2^+$  in our calculations.

LW photons can also be absorbed by hydrogen atoms, through the Lyman series transitions, as discussed in detail by Haiman et al. (1997, 2000). However, this atomic absorption will only have a significant effect on the LW flux over distances large enough that the Hubble expansion causes many of the LW photons to redshift to wavelengths of the Lyman series transitions. The light-crossing time for our cosmological box is much shorter than the Hubble time at the redshifts that we consider. Thus, LW photons will be negligibly redshifted as they cross our cosmological box and we can safely neglect the minimal atomic absorption of these photons that may take place.

It has also been found that a shell of  $\text{H}_2$  molecules may form ahead of the expanding H II regions surrounding the first stars (see Ricotti et al. 2001). These authors find that such shells may become optically thick to LW photons. However, Kitayama et al. (2004) have discussed that such shells are likely short-lived, persisting for only a small fraction of the lifetime of the star. Thus, for our calculations we neglect the possible formation of such a shell, as we expect that the opacity to LW photons through this shell will be very small when averaged over the lifetime of the star. Additionally, as we show in section 3.1, the regions affected by the LW feedback from a single Pop III star extend, at most, only a few kiloparsecs beyond the H II region of such a star, which itself extends  $\sim 5 \text{ kpc}$ . If an  $\text{H}_2$  shell



forms ahead of the H II region, then the extent of the LW bubble will only be suppressed by, at most, a factor of a few in radius.

### 2.3. Sink Particle Formation

We have carried out two simulations, one with radiative feedback and one in which the simulation evolves without including radiative effects. For the former simulation, we allow stars to form when the density reaches  $n_{\text{res}}$ , and the expansion of the gas around the star due to photo-heating suppresses the density so that our resolution limit is not violated. For the simulation without radiative feedback we allow sink particles to form when the density of the gas reaches  $n_{\text{res}}$ . Since the sink particles will form only in minihalos which are expected to form Pop III stars, we are able to track the star formation rate in the case without feedback by tracking the formation of sink particles. We can then compare the sites, and rates, of star formation in each of the simulations in order to elucidate the effect that radiative feedback has on Pop III star formation.

## 3. Results

In this section we discuss the evolution of the primordial gas under the influence of the radiative feedback which arises as the first stars are formed in a region destined to subsequently be incorporated into the first protogalaxy. Indeed, other effects will become important in the course of the buildup of the first galaxies. Among them is the ejection of metals into these systems by the first supernovae (e.g. Bromm et al. 2003). However, we consider the early regime in which Pop III star formation dominates, and the effects of metals might not yet be important. Initially only taking into account the stellar radiative feedback, and neglecting chemical enrichment, relies on our simplifying assumption that only  $100 M_{\odot}$  black hole-forming Pop III stars form, which are predicted not to yield supernovae, and therefore not to eject metals into their surroundings (Heger et al. 2003).

Although the initial mass function (IMF) of the first generation of stars is not known with any certainty yet, there is mounting theoretical evidence that Pop III stars were very massive, and thus it is very likely that many of these stars ended their lives by collapsing directly to black holes, emitting few or no metals into the IGM (see Fryer et al. 2001; Heger et al. 2003). Here we assume that all of the stars that form within our cosmological box are black hole-forming stars which do not enrich the IGM with metals, and which therefore allow subsequent metal-free star formation to occur. Eventually, however, stars which create

supernovae will form, and the ejected metals will be incorporated into the first protogalaxies, thus drawing the epoch of metal-free star formation to a close. In light of this, we end our simulation after the formation of the eighth star in our box at a redshift of  $z \sim 18$ , as we expect that at lower redshifts the effects of the first metals ejected into the primordial gas will become important (but see Jappsen et al. 2007). Also, at lower redshifts global LW feedback, due to star formation at distances far larger than our cosmological box, will become increasingly important. That said, by tracking the formation of individual Pop III stars in our box, we are able to find a variety of novel results concerning the local radiative feedback from the first generations of stars.

### 3.1. The First H II Region and Lyman-Werner Bubble

The first star appears in our cosmological box at a redshift of  $z \sim 23$ . It forms inside a minihalo with a total mass  $\lesssim 10^6 M_\odot$  and the gas within this halo is evaporated due to the photo-heating from the star. The H II region that is formed around the star can be seen in Figure 2, which shows the electron fraction, H<sub>2</sub> fraction, temperature, and density of the gas, in projection. The H II region, which has a morphology similar to those found in previous studies, extends out to  $\sim 4$  kpc from the star, also similar to results found in previous works (Alvarez et al. 2006; Wise et al. 2006; Yoshida et al. 2007).

As shown in Figure 2, the molecules within  $\sim 5$  kpc are photodissociated by the LW radiation from the first star, and the LW bubble extends to only  $\sim 1$  kpc outside of the H II region. Noting that the formation timescale for H<sub>2</sub> in the neutral IGM at these redshifts is of the order of  $\sim 300$  Myr, much longer than the lifetime of the massive stars that we consider here, we can estimate the distance through the IGM that the LW bubble should extend,  $R_{\text{LW}}$ , by evaluating the criterion for the effective dissociation of molecules at this distance from the first star:  $t_{\text{diss,H}_2} = t_*$ . Using equation (8) and taking the lifetime of the star to be 3 Myr gives  $R_{\text{LW}} \sim 5$  kpc, consistent with the result we find for the first star, shown in Figure 2 (see also Ferrara 1998). Outside of this LW bubble molecules will not be dissociated effectively by the single Pop III star, owing largely to its short lifetime. Only when continuous star formation sets in will the LW bubbles of the first generations of stars merge and become large enough to establish a more pervasive LW background flux (see e.g. Haiman et al. 2000).

### 3.2. Thermal and Chemical Evolution of the Gas

The properties of the primordial gas within our box are strongly time-dependent, as any gradual evolution of the gas is disrupted each time a star turns on and heats the gas, ionizes atoms, and photodissociates molecules. Certain robust patterns, however, do emerge in the course of the evolution of the primordial gas. Figure 3 shows the chemical and thermal properties of the gas at a redshift  $z \sim 18$ , just after the death of the eighth star in our cosmological box. Here, the light-shaded particles are those which have been contained within an H II region, and so have passed through a fully ionized phase.

The ionized gas in the H II regions begins to recombine and cool once the central star dies. The dynamical expansion of these hot regions leads to the adiabatic cooling of the gas, as can be seen in the upper left panel of Figure 3. The plot shows relic H II regions at different evolutionary stages. The older ones are generally cooler, owing to the molecular cooling that has had more time to lower the temperature of the gas. Indeed, the first relic H II regions by this redshift,  $\sim 70$  Myr after the first star formed, have already cooled to near the temperature of the un-ionized gas. The electron fraction of the relic H II region gas, however, is still much higher than that of the un-ionized gas, as can be seen in the upper-right panel of Figure 3. That the cooling of the gas occurs faster than its recombination leads to the rapid formation of molecules (e.g. Kang & Shapiro 1992; Oh & Haiman 2003; Nagakura & Omukai 2005; Johnson & Bromm 2006). This elevated fraction of both H<sub>2</sub> and HD molecules in the relic H II region gas is evident in the bottom panels of Figure 3.

The high abundance of molecules in relic H II regions can lead to efficient cooling of the gas, and this has important consequences in the first protogalaxies. In particular, a high fraction of HD in these regions could allow the gas to cool to the temperature of the cosmic microwave background (CMB),  $T_{\text{CMB}}$ , the lowest temperature attainable by radiative cooling, and this effective cooling may lead to the formation of lower mass metal-free stars (Nagakura & Omukai 2005; Johnson & Bromm 2006; Yoshida 2006). Indeed, Figure 3 shows that the HD fraction can greatly exceed the minimum value needed for efficient cooling to the CMB temperature floor in local thermodynamic equilibrium (LTE),  $f_{\text{HD,crit}} \sim 10^{-8}$  (Johnson & Bromm 2006).

While the LW feedback from the stars that form in our box can very effectively destroy molecules within  $\sim 5$  kpc of the stars by the end of their lives, this feedback is not continuous. Following the death of a given star, the molecules will begin to reform in the absence of LW radiation. The time required for the formation of H<sub>2</sub> molecules is sensitively dependent on the ionized fraction of the gas, but the formation time can be relatively short for un-ionized gas at high densities, as well. In relic H II regions the fraction of H<sub>2</sub> can reach  $10^{-4}$  within  $\sim 1$  Myr (Johnson & Bromm 2007). In collapsing minihalos, where the molecules play a

key role in cooling the gas and allowing it to continue collapsing, the formation times are in general longer at the densities we consider here,  $n \lesssim 20 \text{ cm}^{-3}$ . We find that the formation timescale for un-ionized gas collapsing in minihalos is  $t_{\text{form,H}_2} \sim 5 \times 10^5 \text{ yr}$  at a density of  $1 \text{ cm}^{-3}$  and a temperature of 900 K, and  $t_{\text{form,H}_2} \sim 7 \times 10^6 \text{ yr}$  at a density of  $0.1 \text{ cm}^{-3}$  and a temperature of 500 K. The average time between the formation of stars in our box is  $\sim 10 \text{ Myr}$ , and so the molecules inside sufficiently dense minihalos can often reform and allow the gas to continue cooling and collapsing, in spite of the intermittent LW feedback from local star forming regions.

In order to evaluate the possible effects of continuous LW feedback from sources outside of our box, we have carried out simulations in which we include a LW background which destroys  $\text{H}_2$  molecules at a rate given by (Abel et al. 1997)

$$k_{\text{diss}} = 1.2 \times 10^{-12} J_{\text{LW}} \text{ s}^{-1}, \quad (14)$$

where  $J_{\text{LW}}$  is the flux of LW photons in units of  $10^{-21} \text{ ergs s}^{-1} \text{ cm}^{-2} \text{ Hz}^{-1} \text{ sr}^{-1}$ . We have carried out simulations in which the value of  $J_{\text{LW}}$  is taken to be zero before the formation of the first star and 0.1,  $10^{-2}$ , and  $10^{-3}$  afterwards, when a LW background might be expected to begin building up due to distant star formation. For each of these simulations, we found the formation redshift of the second star in the box to be  $z_{2\text{nd}} = 16.3, 20,$  and  $20.5$ , respectively. In our main simulation, in which we neglect a possible background LW flux, the second star formed at  $z_{2\text{nd}} = 20.6$ . This demonstrates that a background LW flux of  $J_{\text{LW}} \lesssim 10^{-2}$  would likely have little impact on our results, while a larger LW flux would simply delay the collapse of gas into minihalos and so lower the overall star formation rate in our box, consistent with previous findings (see e.g. Machacek et al. 2001; Mesinger et al. 2006). We emphasize, however, that for a substantial LW background to be established, a relatively high continuous star formation rate must be achieved, as we have shown that individual Pop III stars can only be expected to destroy molecules within  $\sim 5 \text{ kpc}$  of their formation sites. In the very early stages of the first star formation, when short-lived single stars are forming in individual minihalos (see e.g. Yoshida et al. 2006), it appears unlikely that a substantial LW background would be established, the feedback from the sources being instead largely local. It may be only later, when continuous star formation begins to occur in larger mass systems that a pervasive LW background would likely be built up (see, e.g., Haiman et al. 2000; Greif & Bromm 2006).

### 3.3. Shielding of Molecules by Relic H II Regions

As star formation continues, the volume occupied by relic H II regions increases. Because of the high molecule fraction that can develop in these regions, owing to the large electron fraction that persists for  $\lesssim 500$  Myr (Johnson & Bromm 2007), the increasing volume of the IGM occupied by relic H II regions implies an increase in the optical depth to LW photons in the vicinity of the first star formation sites. By a redshift of  $z \sim 18$ , eight stars have formed in our cosmological box and each has left behind a relic H II region.

As can be seen in Figures 3 and 4, the gas inside the relic H II regions that have formed contains an  $\text{H}_2$  fraction generally higher than the primordial abundance of  $10^{-6}$ , and up to an abundance of  $\sim 10^{-3}$  in the denser regions. This elevated fraction of  $\text{H}_2$  inside the relic H II regions leads to a high optical depth to LW photons,  $\tau_{\text{LW}}$ , through the relic H II regions. The column density through a relic H II region which recombines in the absence of LW radiation can become of the order of  $N_{\text{H}_2} \sim 10^{15} \text{ cm}^{-2}$  (Johnson & Bromm 2007). Because the molecules in the relic H II regions that we consider here are subject to LW feedback from neighboring star formation regions, the optical depth through these regions may in general be lower. However, the rapid rate of molecule formation in these regions, even considering the LW feedback from local star forming regions in our box, allows the molecule fraction to approach  $10^{-4}$  as late as  $\sim 100$  Myr after the death of the central star. This elevated molecule fraction combined with the growing volume-filling fraction of relic H II regions leads to an appreciable optical depth to LW photons, which generally increases with time as more stars form and create more relic H II regions. To quantify this effect, we calculate the average column density of  $\text{H}_2$  molecules through a cubic region of side length  $l$  as the product of the length  $l$  and the volume averaged number density of  $\text{H}_2$  molecules, given by

$$N_{\text{H}_2} \simeq l \frac{\sum n_{\text{H}_2} V}{\sum V}, \quad (15)$$

where the sum is over all of the SPH particles in the volume and  $n_{\text{H}_2}$  is the number density of  $\text{H}_2$  at each of the SPH particles. The volume associated with each individual SPH particle,  $V$ , is estimated as  $V \simeq m_{\text{SPH}}/\rho$ , where  $m_{\text{SPH}}$  is the mass of the SPH particle and  $\rho$  is the mass density of the gas at that particle. The optical depth to LW photons is then computed as (Draine & Bertoldi 1996; Haiman et al. 2000)

$$\tau_{\text{LW}} \simeq 0.75 \ln\left(\frac{N_{\text{H}_2}}{10^{14} \text{ cm}^{-2}}\right). \quad (16)$$

Figure 5 shows the optical depth to LW photons averaged both over the central co-

moving  $153 \text{ kpc } h^{-1}$  of our cosmological box, in which the first star forms, and over the entire box, for which the comoving side length is  $460 \text{ kpc } h^{-1}$ . Before the formation of the first star, the optical depth evolves largely owing to the cosmic expansion, following the relation  $\tau_{\text{LW}} \simeq n_{\text{H}_2} l \propto (1+z)^2$ , because the average  $\text{H}_2$  fraction does not change appreciably. However, with the formation of the first star in our box at  $z \simeq 23$  the optical depth begins to change dramatically in the inner portion of the box, first falling to a value of  $\simeq 0.1$  due to the LW feedback from the first star and then steadily climbing to values  $\gtrsim 2$  as copious amounts of molecules form inside the relic H II regions that accumulate as star formation continues.

The evolution of the optical depth averaged over the entire box is not as dramatic, as the fraction of the volume of the whole box occupied by relic H II regions is much smaller than the fraction of the central region that is occupied by these molecule-rich regions. However, the optical depth averaged over the whole box, which is a better estimate of the optical depth over cosmological distances, still rises to  $\tau_{\text{LW}} \gtrsim 1.5$  across our box, an appreciable value which will serve to impede the build-up of a cosmologically pervasive LW background.

### 3.4. Black hole accretion

Accretion onto Pop III relic black holes may be inefficient for some time following the formation of these objects, owing to the fact that Pop III stars photo-heat and evaporate the gas within the minihalos which host them (Johnson & Bromm 2007; see also Yoshida 2006). Indeed, accretion onto Pop III relic black holes at close to the Eddington limit can only occur if the accreted gas has a density above  $\sim 10^2 \text{ cm}^{-3}$ , and it is only in collapsing halos that such densities are achieved at the high redshifts at which the first stars formed (Johnson & Bromm 2007). By assumption, all of the stars that are formed in our simulation are black hole-forming Pop III stars. If these black holes remain inside their host minihalos, then by tracking the evolution of the gas within these photo-evaporated host minihalos, we can learn when efficient accretion onto these Pop III relic black holes may occur.

The minihalo within which the first star forms at a redshift  $z \sim 23$  resides within the relic H II region left by the first star. Due to the formation of a high fraction of molecules, and to the molecular cooling that ensues, the relic H II region gas cools down to temperatures  $\sim 10^3 \text{ K}$ , below the virial temperature of this  $10^6 M_\odot$  minihalo. The gas then re-collapses into the minihalo, reaching a peak density of  $n_{\text{res}}$  at a redshift  $z \sim 19$ , or  $\sim 50 \text{ Myr}$  after the formation of the first star. Figure 6 shows the properties of the relic H II region gas as a function of distance from the center of this minihalo, at the time when the gas has collapsed to a density of  $n_{\text{res}}$ . We cannot, with this simulation, resolve what happens once

the gas collapses further and reaches higher densities. However, we can estimate the time it will take for the gas at the center of the halo to reach a density of  $n \sim 10^2 \text{ cm}^{-3}$  as the free fall time of the gas, which is  $t_{\text{ff}} \sim 10 \text{ Myr}$ . Thus, a Pop III relic black hole at the center of this halo could be expected to begin accreting gas efficiently  $\sim 60 \text{ Myr}$  after its formation. This is a significant delay, and could pose serious challenges to theories which predict that efficient accretion onto Pop III relic black holes can lead to these black holes becoming the supermassive black holes that power the quasars observed in the *Sloan Digital Sky Survey* at redshifts  $z \gtrsim 6$  (e.g. Yoshida 2006; Johnson & Bromm 2007; Li et al. 2006).

### 3.5. HD cooling in relic H II regions

While abundant molecules can form within relic H II regions, the LW feedback from neighboring star-forming regions can suppress the effect of this elevated fraction of molecules. The electron fraction remains high in relic H II regions for up to  $\sim 500 \text{ Myr}$  in the general IGM, but in higher density regions where the gas is recollapsing, the electron fraction drops much more quickly. Figures 3 and 6 show that the electron fraction drops to a value of  $\lesssim 10^{-4}$ , comparable to the electron fraction of the un-ionized gas, once the density of the relic H II region gas becomes  $\gtrsim 10 \text{ cm}^{-3}$ . Thus, once the gas reaches these densities the ionized fraction will become too low to catalyze the formation of a high fraction of molecules, and of HD molecules in particular. Therefore, in order for HD to be an effective coolant of the primordial gas in relic H II regions, the abundant HD molecules that are formed at densities  $\lesssim 10 \text{ cm}^{-3}$  must not be destroyed by LW feedback from neighboring star-forming regions before the gas collapses to high densities and forms stars. If we estimate the timescale on which the relic H II region gas would collapse to form stars as the free-fall time of the gas, we find that the molecules must be shielded from photodissociating radiation for at least  $t_{\text{ff}} \gtrsim 10 \text{ Myr}$  in order for the high abundance of HD molecules to persist, so that the formation of so-called Pop II.5 stars might be enabled, with their hypothesized masses of  $\sim 10 M_{\odot}$  (see Johnson & Bromm 2006).

We find that the relic H II region gas that re-collapses into the minihalo in which the first star formed, shown in Figure 6, carries a high fraction of HD molecules, as LW feedback from neighboring stars does not effectively dissociate the molecules in this relatively dense and self-shielded gas. The HD fraction exceeds  $10^{-7}$ , becoming an order of magnitude higher than its value for un-ionized primordial gas collapsing in a minihalo. Thus, for this case, HD cooling will likely be effective at higher densities as the gas collapses further, and we expect that a Pop II.5 star, with a mass of the order of  $10 M_{\odot}$ , might form later on, if we were to run the simulation further (Nagakura & Omukai 2005; Yoshida 2006; Johnson & Bromm

2006; Yoshida et al. 2007). Had star formation taken place nearer this minihalo between the formation of the first star and the re-collapse of the gas into the host minihalo, then the molecule fraction would likely not be so elevated, and a higher mass metal-free star would be more likely to form. Thus, while in our simulation it appears that the first relic H II region that forms may give rise to Pop II.5 star formation, we emphasize that the possibility of the formation of Pop II.5 stars in relic H II regions is very dependent on the specific LW feedback that affects the gas in these regions.

### 3.6. Star Formation in the Presence of Radiative Feedback

To discern the effect the local radiative feedback from the first stars has on the star formation rate, we have compared the results obtained from our simulations with and without radiative feedback. By a redshift of  $z \sim 18$ , a total of nine star-forming regions were identified in our simulation without feedback, while at the same epoch eight stars had formed in our simulation including feedback. Thus, we find that the average star formation rate at redshifts  $z \gtrsim 18$  is diminished by a factor of perhaps only  $\lesssim 20$  percent due to local radiative feedback, although this result is subject to the small number statistics within our single cosmological box. Figure 7 shows the locations of the sites of star formation for both cases, plotted in comoving coordinates against the projected density field. The orange squares denote sites where Pop III stars could have formed in the case without feedback, while the green dots denote sites where Pop III stars formed in the simulation including radiative feedback. Thus, the sites where star formation is suppressed by the radiative feedback are marked by the orange squares which are not filled by a green dot.

We point out, however, that we do not include LW feedback from stars which may have formed outside of our box, and hence it is possible that the overall LW feedback may be stronger than we find here. At redshift  $z \sim 18$ , we end the simulation, but note that star formation will likely take place at an increasing rate as the collapse fraction increases with time. This could lead to a continuous LW background produced within our box, different from the intermittent LW feedback produced by individual stars that occurs in the simulation down to  $z \sim 18$ .

Also, the limits of our resolution prohibit us from discerning the stronger shielding of H<sub>2</sub> molecules and I-front trapping that could occur within very dense collapsing minihalos (see Ahn & Shapiro 2006). However, we note that these authors find that the radiative feedback on collapsing minihalos from nearby stars generally does not greatly affect the final outcome of the collapse, as halos which collapse in the absence of radiative feedback generally also collapse when radiative feedback is applied (see also Susa & Umemura 2006),



roughly consistent with our results in the present work. Thus, our limited resolution may not substantially impact the results that we find for the slight suppression of star formation due to local radiative feedback, although higher resolution simulations will be necessary to more precisely study the full impact of radiative feedback from the first stars on the first protogalaxies.

#### 4. Summary and Discussion

We have performed cosmological simulations which self-consistently account for the radiative feedback from individual Pop III stars, as they form in the course of the assembly of the first protogalaxies. We have solved in detail for the H II regions, as well as for the LW bubbles of these stars, wherein molecule-dissociating radiation effectively destroys H<sub>2</sub> and HD molecules. The local radiative feedback from the first stars is complex, and we find a variety of novel results on the evolution of the primordial gas, on the effects of the LW radiation from the first stars, on the nature of second generation star formation, and on black hole accretion.

While the LW radiation from the first stars can, in principle, greatly suppress Pop III star formation in the early universe, we find that a number of factors minimize the effectiveness of this negative feedback. Firstly, the LW radiation produced locally by individual stars is not uniform and constant, as LW feedback has been modeled in previous work (e.g., Ciardi & Ferrara 2005; Mesinger et al. 2006), but rather is present only during the brief lifetimes of the individual stars that produce it. Thus, even if the molecules in collapsing minihalos and relic H II regions are destroyed by the radiation from individual stars, they will, at the early stages of Pop III star formation, have time to reform and continue cooling the primordial gas in between the times of formation of local stars. Furthermore, because the LW bubbles of individual Pop III stars extend only to  $R_{LW} \sim 5$  kpc from these sources, due to the short stellar lifetimes, the build up of a pervasive LW background would likely have to await the epoch of continuous star formation, which is fundamentally different from the epoch of the first stars, in which these sources shine for short periods within individual minihalos.

As star formation continues, the volume-filling fraction of relic H II regions increases as well, and this, combined with the high fraction of molecules that form in these regions, leads to an opacity to LW photons through the IGM which increases with time. This opacity can become of the order of  $\tau_{LW} \gtrsim 2$  through individual relic H II regions (Johnson & Bromm 2007; see also Ricotti et al. 2001; Machacek et al. 2001, 2003; Oh & Haiman 2002). Furthermore, as the volume-filling fraction of relic H II regions increases with time,  $\tau_{LW}$  through the general IGM may become similarly large, and this effect will have to be considered in future work

which seeks to elucidate the effect of LW feedback on Pop III star formation.

We find that metal-free stars with masses of the order of  $10 M_{\odot}$ , the postulated Pop II.5 stars (e.g. Johnson & Bromm 2006; Greif & Bromm 2006), might form from the molecule-enriched gas within the first relic H II regions, although we note that this may not occur in general, due to LW feedback from neighboring star-forming regions. This susceptibility to LW feedback is due to the fact that the high fraction of HD molecules which forms in the electron-rich, low density regions of relic H II regions must persist until this gas has had time to collapse to high densities and form stars. If LW feedback from neighboring star-forming regions destroys the molecules after the gas has collapsed to densities  $\gtrsim 10 \text{ cm}^{-3}$ , then the abundance of HD molecules will not likely be elevated when the gas forms stars and Pop II.5 star formation may be suppressed. Because this implies that the molecules must be shielded from LW radiation for, at least, the free-fall time for gas with densities  $\lesssim 10 \text{ cm}^{-3}$ , or  $\gtrsim 10 \text{ Myr}$ , we conclude that Pop II.5 star formation in relic H II regions may occur only in the circumstances when local Pop III star formation is suppressed over such timescales. However, we also point out that the shielding provided by the high  $\text{H}_2$  fraction in these relic H II regions may help to minimize the LW feedback from neighboring star-forming regions, and so may make Pop II.5 star formation in relic H II regions possible in many cases.

We find that the ionized primordial gas surrounding the first star formed in our simulation, at a redshift of  $z \sim 23$ , recombines and cools by molecular cooling to temperatures below the virial temperature of the minihalo that hosted this first star. Thus, this relic H II region gas is able to re-collapse to densities  $\gtrsim 20 \text{ cm}^{-3}$  within this minihalo after  $\sim 50 \text{ Myr}$  from the death of the star. It is predicted that many Pop III stars will collapse directly to form black holes with masses of the order of  $100 M_{\odot}$  (e.g. Heger et al. 2003), and if such a black hole resides within this host halo, then we find that it may begin accreting dense primordial gas at close to the Eddington rate after  $\sim 60 \text{ Myr}$  from the time of its formation. This is an important consideration to be incorporated into models of the growth of the  $10^9 M_{\odot}$  black holes which have been observed at redshifts  $\gtrsim 6$ , as it places constraints on the amount of matter that a given relic Pop III black hole could accrete by this redshift (e.g. Haiman & Loeb 2001; Volonteri & Rees 2006; Li et al. 2006).

Finally, by comparing the star formation rates which we derive from our simulation including radiative feedback with those derived from our simulation in which feedback is left out, we have seen that local radiative feedback from the first stars likely only diminishes the Pop III star formation rate by a factor of, at most, a few. In our simulation, in particular, we find that this rate is decreased by only  $\lesssim 20$  percent, although this may be less suppression than would be expected by the overall radiative feedback, as we did not include the possible effects of a global LW background. Future simulations which resolve densities higher than

those reached here, and which self-consistently track the build-up of the LW background along with the IGM opacity to LW radiation, will be necessary to more fully explore the radiative effects of the first stars on the formation of the first galaxies. However, the goal of understanding the formation of the first galaxies is now clearly getting within reach, and the pace of progress is expected to be rapid.

We would like to thank Yuexing Li and Kyungjin Ahn for helpful discussions. We are also grateful to Simon Glover and the anonymous referee for valuable comments that improved the quality of this work. The simulations used in this work were carried out at the Texas Advanced Computing Center (TACC).

## REFERENCES

- Abel, T., Anninos, P., Zhang, Y., & Norman, M. L. 1997, *New Astro.*, 3, 181
- Abel, T., Bryan, G. L., & Norman, M. L. 2002, *Science*, 295, 93
- Abel, T., Wise, J. H., & Bryan, G. L. 2006, *ApJ*, submitted (astro-ph/0606019)
- Ahn, K., & Shapiro, P. R. 2006, *MNRAS*, in press (astro-ph/0607642)
- Alvarez, M. A., Bromm, V., & Shapiro, P. R. 2006, *ApJ*, 639, 621
- Barkana, R., & Loeb, A. 2001, *Phys. Rep.*, 349, 125
- Beers, T. C., & Christlieb, N. 2005, *ARA&A*, 43, 531
- Bouwens, R. J., & Illingworth, G. D. 2006, *Nature*, 443, 189
- Bromm, V., Coppi, P. S., & Larson, R. B. 1999, *ApJ*, 527, L5
- Bromm, V., Coppi, P. S., & Larson, R. B. 2002, *ApJ*, 564, 23
- Bromm, V., Kudritzki R. P., & Loeb A. 2001, *ApJ*, 552, 464
- Bromm, V., & Loeb, A. 2003, *ApJ*, 596, 34
- Bromm, V., Yoshida, N., & Hernquist, L. 2003, *ApJ*, 596, L135
- Bromm, V., & Larson, R. B. 2004, *ARA&A*, 42, 79
- Christlieb, N. et al. 2002, *Nature*, 419, 904

- Ciardì, B., & Ferrara, A. 2005, *Space Sci. Rev.*, 116, 625
- Ciardì, B., Ferrara, A., Governato, F., & Jenkins, A. 2000, *MNRAS*, 314, 611
- Ciardì, B., Scannapieco, E., Stoehr, F., Ferrara, A., Iliev, I. T., & Shapiro, P. R. 2006, *MNRAS*, 366, 689
- Davé, R., Finlator, K., & Oppenheimer, B. D. 2006, *MNRAS*, 370, 273
- de Jong, T. 1972, *A&A*, 20, 263
- Draine, B. T., & Bertoldi, F. 1996, *ApJ*, 468, 269
- Dunn, G. H. 1968, *Phys. Rev.*, 172, 1
- Fan, X. et al. 2004, *AJ*, 128, 515
- Fan, X. et al. 2006, *AJ*, 131, 1203
- Ferrara, A. 1998, *ApJ*, 499, L17
- Frebel, A. et al. 2005, *Nature*, 434, 871
- Fryer, C. L., Woosley, S. E., & Heger, A. 2001, *ApJ*, 550, 372
- Galli, D., & Palla, F. 1998, *A&A*, 335, 403
- Gao, L., Abel, T., Frenk, C. S., Jenkins, A., Springel, V., & Yoshida, N. 2007, *MNRAS*, submitted (astro-ph/0610174)
- Gardner, J. P. et al. 2006, *Space Sci. Rev.*, 123, 485
- Glover, S. C. O., & Brand, P. W. J. L. 2001, *MNRAS*, 321, 385
- Greif, T., Bromm, V. 2006, *MNRAS*, 373, 128
- Heger, A., Fryer, C. L., Woosley, S. E., Langer, N., & Hartmann, D. H. 2003, *ApJ*, 591, 288
- Haiman, Z., Abel, T., & Rees, M. J. 2000, *ApJ*, 534, 11
- Haiman, Z., & Loeb, A. 2001, *ApJ*, 552, 459
- Haiman, Z., Rees, M. J., & Loeb, A. 1996, *ApJ*, 467, 522
- Haiman, Z., Rees, M. J., & Loeb, A. 1997, *ApJ*, 476, 458
- Iye, M., et al. 2006, *Nature*, 443, 186

- Jappsen, A.-K., Glover, S. C. O., Klessen, R. S., MacLow M.-M. 2007, *ApJ*, accepted (astro-ph/0511400)
- Jimenez, R., & Haiman, Z. 2006, *Nature*, 440, 501
- Johnson, J. L., & Bromm, V. 2006, *MNRAS*, 366, 247
- Johnson, J. L., & Bromm, V. 2007, *MNRAS*, 374, 1557
- Kang, H., & Shapiro, P. R. 1992, *ApJ*, 386, 432
- Karpas, Z., Anicich, V., & Huntress, W. T. 1979, *J. Chem. Phys.*, 70, 2877
- Kawata, D., Arimoto, N., Cen, R., & Gibson, B. K. 2006, *ApJ*, 641, 785
- Kitayama, T., Yoshida, N., Susa, H., & Umemura, M. 2004, *ApJ*, 613, 631
- Li, Y., et al. 2006, *ApJ*, submitted (astro-ph/0608190)
- Machacek, M. E., Bryan, G. L., & Abel, T. 2001, *ApJ*, 548, 509
- Machacek, M. E., Bryan, G. L., & Abel, T. 2003, *MNRAS*, 338, 273
- Mackey, J., Bromm, V., & Hernquist, L. 2003, *ApJ*, 586, 1
- Mesinger, A., Bryan, G. L., & Haiman, Z. 2006, *ApJ*, 648, 835
- Mobasher, B., et al. 2005, *ApJ*, 635, 832
- Nagakura, T., & Omukai, K. 2005, *MNRAS*, 364, 1378
- Oh, P., & Haiman, Z. 2002, *ApJ*, 569, 558
- Oh, P., & Haiman, Z. 2003, *MNRAS*, 346, 456
- O’Shea, B. W., Abel, T., Whalen, D., & Norman, M. L. 2005, *ApJ*, 628, L5
- Palla, F. 2002, in *Physics of Star Formation in Galaxies*, ed. A. Maeder & G. Meynet (Berlin: Springer)
- Ricotti, M., Gnedin, N. Y., & Shull, J. M. 2001, *ApJ*, 560, 580
- Schaerer, D. 2002, *A&A*, 382, 28
- Spergel, D. N., et al. 2003, *ApJS*, 148, 175
- Springel, V., Yoshida, N., & White, S. D. M. 2001, *NewA*, 6, 79

- Springel, V., & Hernquist, L. 2002, MNRAS, 333, 649
- Susa, H., & Umemura, M., 2006, ApJ, 645, L93
- Tassis, K., Abel, T., Bryan, G. L., & Norman, M. l. 2003, ApJ, 587, 13
- Tassis, K., Kravtsov, A. V., & Gnedin, N. Y. 2006, ApJ, submitted (astro-ph/0609763)
- Volonteri, M., & Rees, M. J. 2006, ApJ, 650, 669
- Whalen, D., Abel, T., & Norman, M. L. 2004, ApJ, 610, 14
- Yoshida, N. 2006, NewA Rev., 50, 19
- Yoshida, N., Oh, S. P., Kitayama, T., & Hernquist, L. 2007, ApJ, submitted (astro-ph/0610819)
- Yoshida, N., Omukai, K., Hernquist, L., & Abel, T. 2006, ApJ, 652, 6

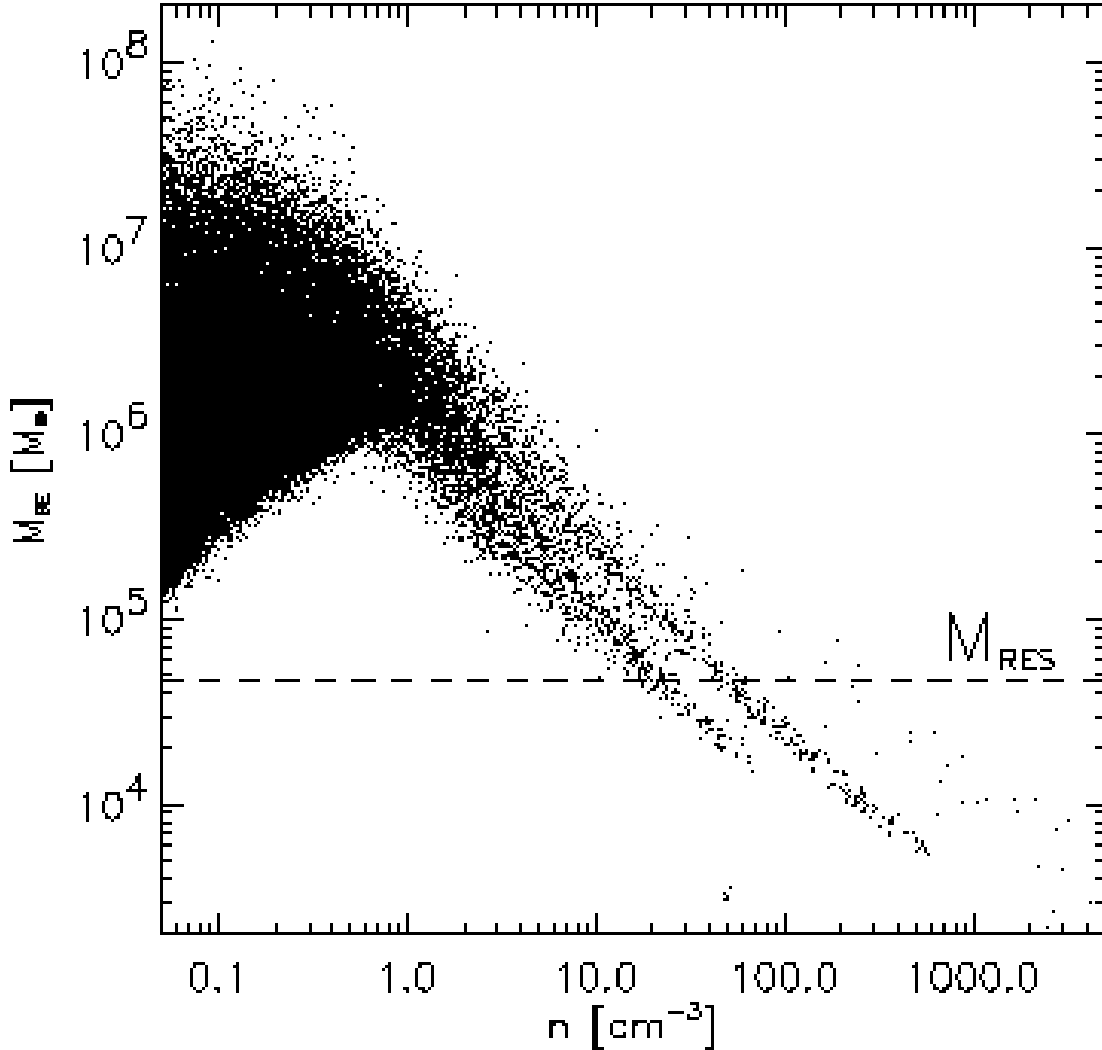


Fig. 1.— Determining the maximum density resolvable in our simulations. To reliably resolve the properties of the gas in our simulation, the Bonnor-Ebert mass, similar to the Jeans mass, must be larger than the mass in the SPH smoothing kernel. For added assurance, we take the minimum resolvable mass to be twice the mass in the kernel. This value for the resolution mass is shown by the dashed horizontal line. For densities higher than  $n_{\text{res}} \sim 20 \text{ cm}^{-3}$ , the Bonnor-Ebert mass may be exceeded by the resolution mass, and so we take it that we can only resolve the properties of the gas at densities below this value. We note that the two structures emerging at high densities are two spatially distinct halos of different mass which are undergoing collapse.

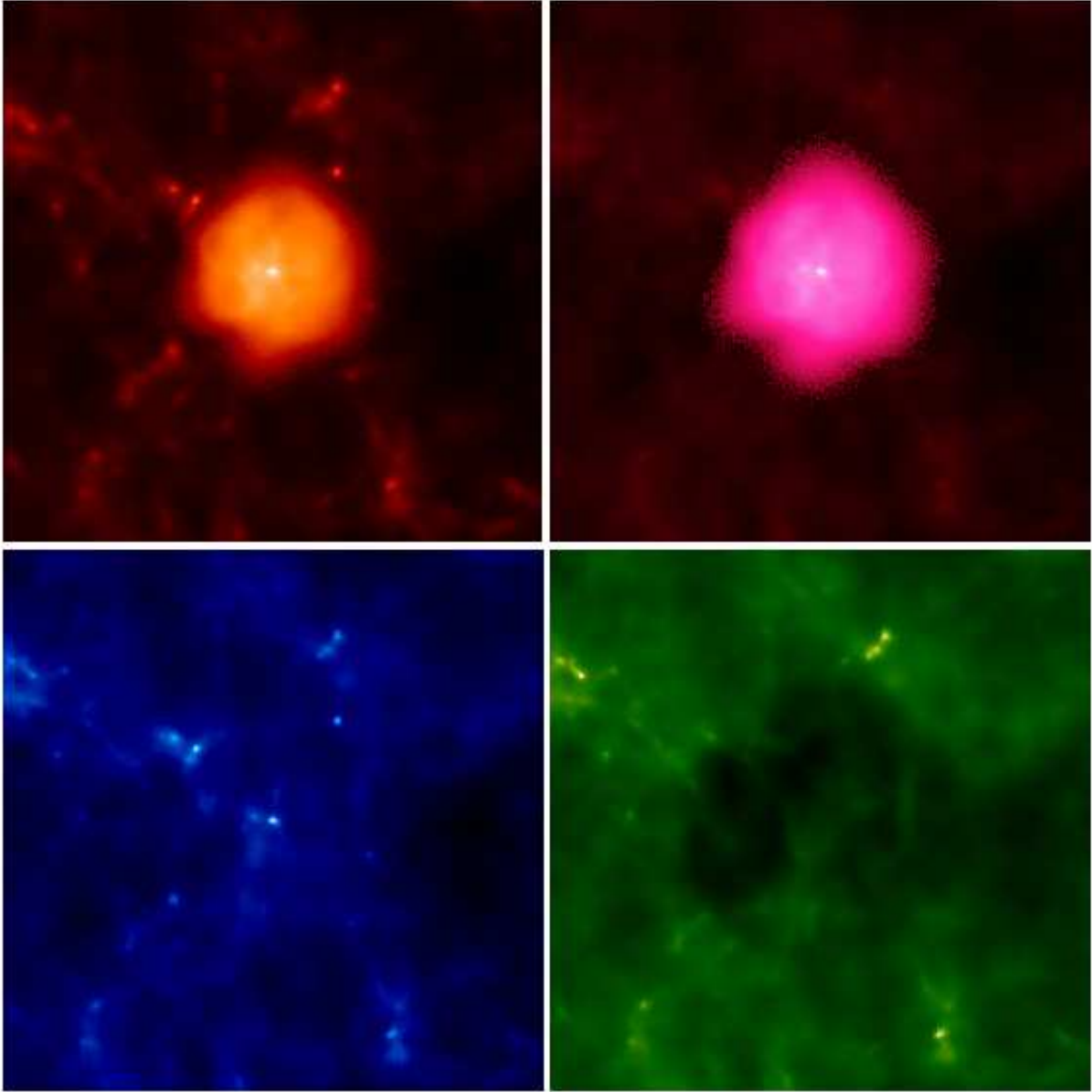


Fig. 2.— The first H II region and LW bubble. Clockwise from top-left are the temperature, electron fraction,  $\text{H}_2$  fraction, and density, plotted in projection. While the size of our cosmological box is  $\sim 27$  kpc in physical units at this redshift,  $z \sim 23$ , here we have zoomed into the inner 20 kpc, in order to see detail around the first star. The H II region extends out to  $\sim 4$  kpc in radius, while the LW bubble extends to  $\sim 5$  kpc, within which the molecule fraction is zero. In each panel, the lighter shades signify higher values of the quantity plotted.



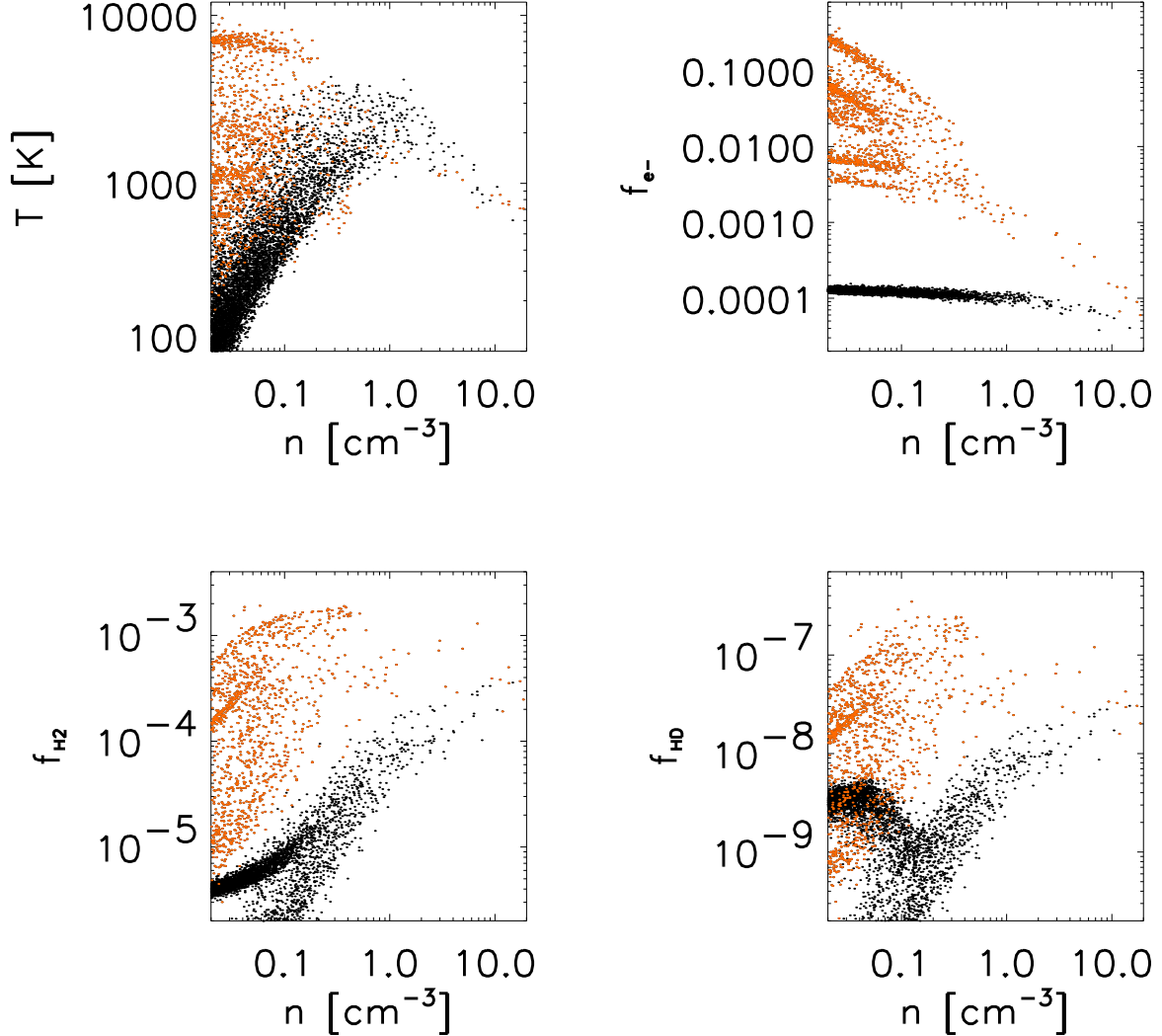


Fig. 3.— The properties of the primordial gas at redshift  $z \sim 18$ , at the end of the life of the eighth star. The SPH particles which have experienced an ionized phase within an H II region are colored in orange (gray), while those that have not are in black. Clockwise from the top-left, the temperature, free electron fraction, HD fraction, and  $\text{H}_2$  fraction are plotted as functions of gas density. The relic H II region gas cools largely by adiabatic expansion, but, importantly, also by cooling facilitated by the high abundance of  $\text{H}_2$  and HD molecules, which arises owing to the high electron fraction in this gas. The high electron fraction persists until the gas has collapsed to densities of  $\gtrsim 10 \text{ cm}^{-3}$ , as can be seen in the top-right panel. The molecule fraction is highest at low densities for gas in which the molecules have not been destroyed by LW feedback, giving rise to the features seen at low densities in the bottom two panels.

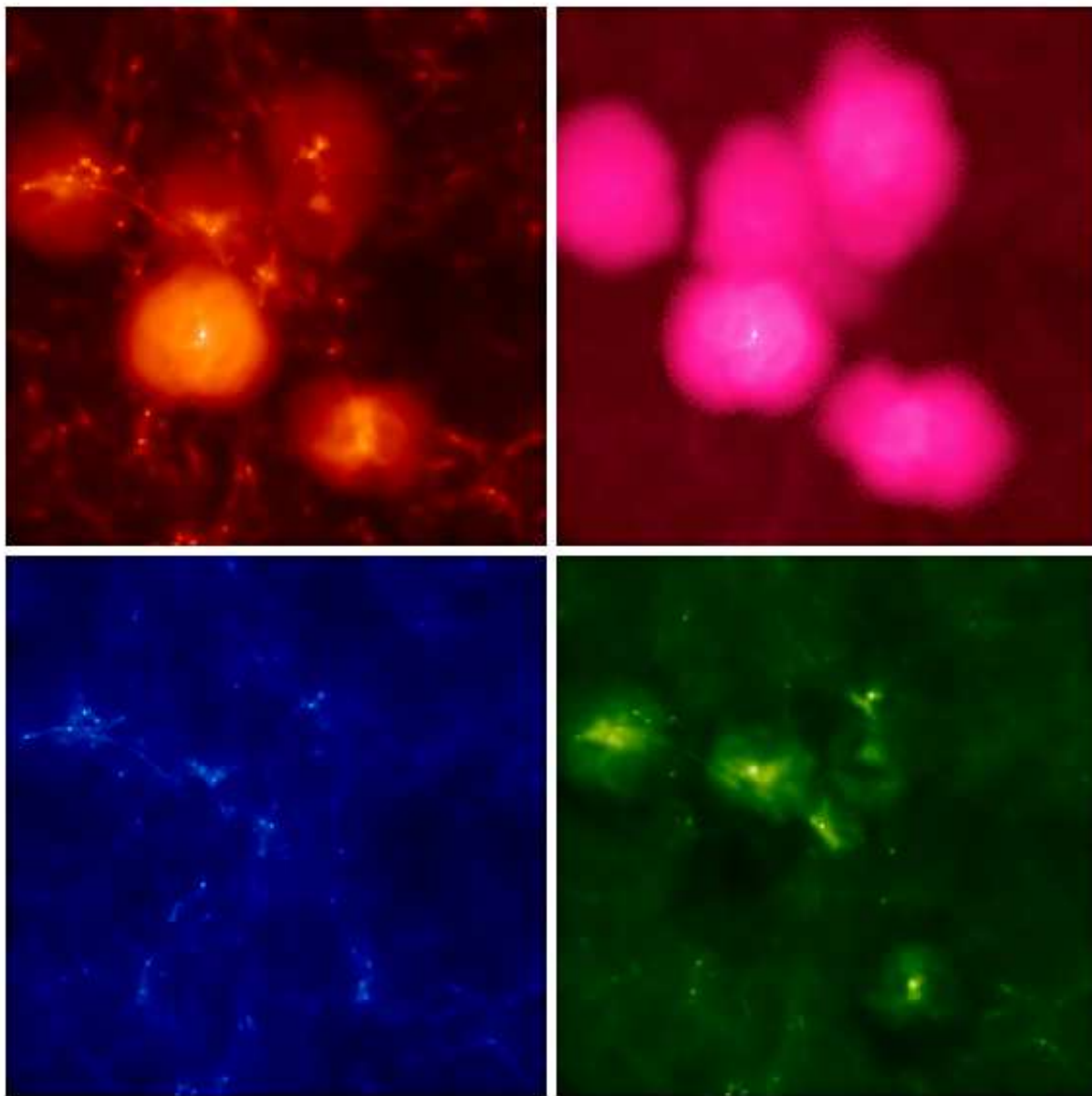


Fig. 4.— The properties of the primordial gas at the end of the life of the eighth star in our box, at redshift  $z \sim 18$ . Clockwise from top-left are the temperature, electron fraction,  $\text{H}_2$  fraction, and density of the gas, in projection. Here we show the entire cosmological box, which is  $\sim 35$  kpc in physical units. Note the high electron and  $\text{H}_2$  fractions in the relic H II regions, where recombination is taking place. The elevated  $\text{H}_2$  fraction in these regions raises the optical depth to LW photons through them significantly, as is illustrated in Fig. 5. The temperature in the older relic H II regions is not greatly elevated as compared to the temperature of the un-ionized gas, owing to the adiabatic and molecular cooling that takes place in these regions. The lighter shades denote higher values of the quantities plotted.

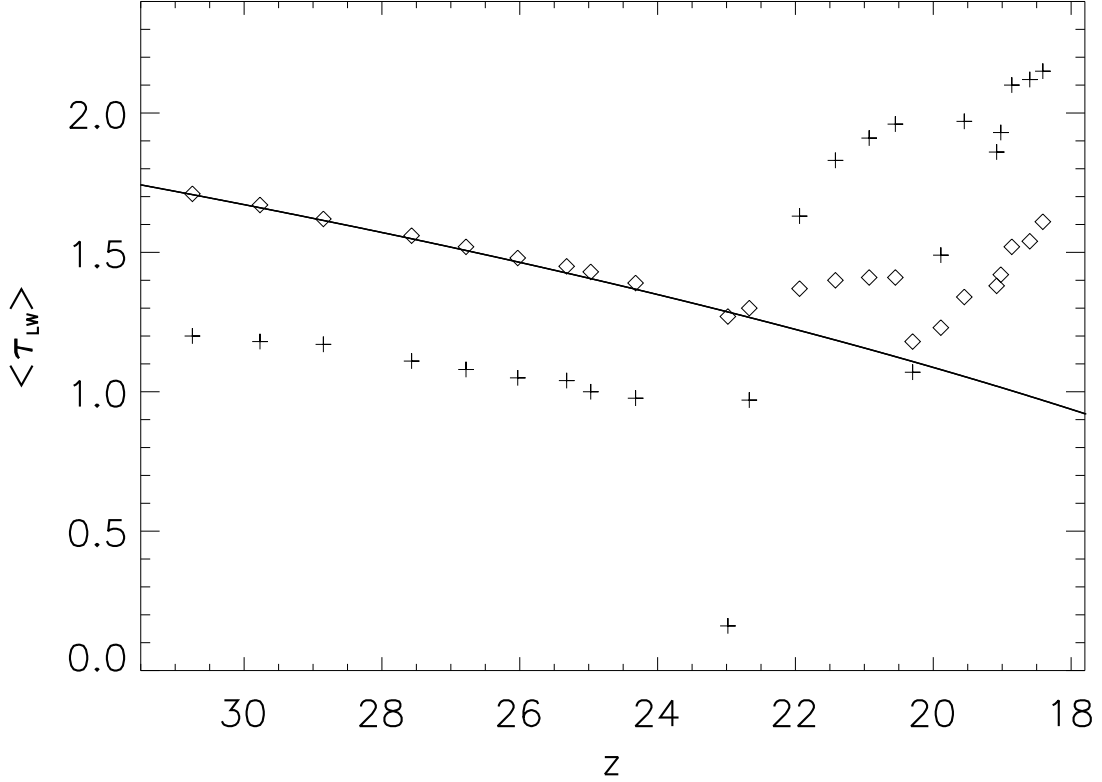


Fig. 5.— The optical depth to LW photons,  $\tau_{LW}$ , averaged over two volumes in our box, as a function of redshift,  $z$ . The diamonds denote the optical depth averaged over the entire cosmological box, while the crosses denote the optical depth averaged only over a cube containing the inner comoving  $153 \text{ kpc } h^{-1}$  of the box, centered in the middle of the box with a volume one ninth that of the whole box. It is within this region that the first star forms and the star formation rate is higher than the average star formation rate over the whole box, and this is reflected in the higher local optical depth in this region as relic H II regions accumulate in the box. The average optical depth through the entire box also rises, but the increase is less dramatic. The solid line denotes the optical depth to LW photons, averaged over the whole box, that would be expected for the case that the gas maintains the average cosmological density everywhere and that the  $\text{H}_2$  fraction does not change from the primordial value of  $2 \times 10^{-6}$ ; for this case, the optical depth changes owing only to cosmic expansion. Note that the optical depth averaged over the whole box matches well this idealized case up until the first star forms at a redshift of  $z \sim 23$ . The temporary drops in the optical depth occur due to LW feedback when individual stars form.

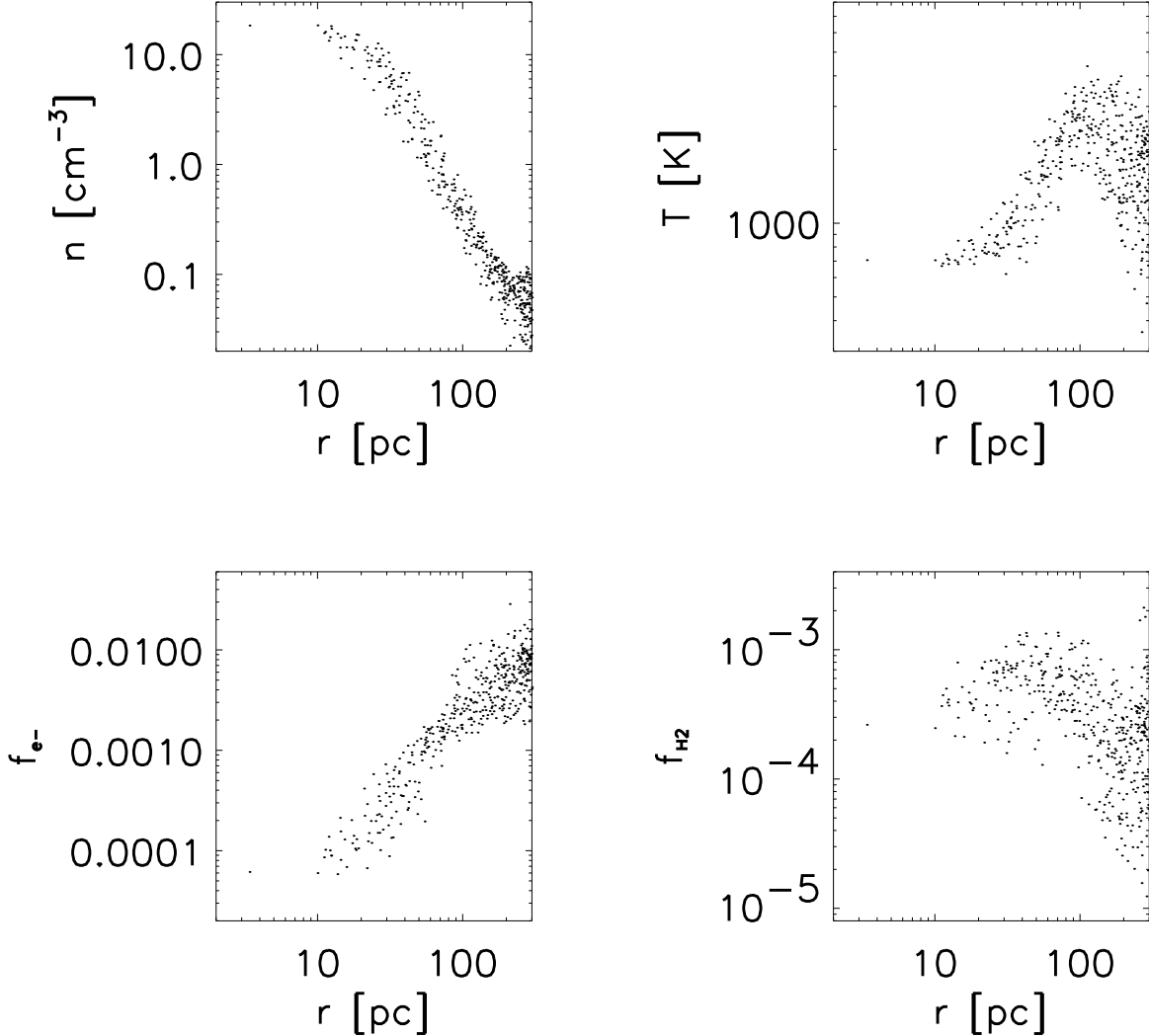


Fig. 6.— The properties of the relic H II region gas which recollapses into the minihalo which hosted the first star. Clockwise from the top-left are the density, temperature, H<sub>2</sub> fraction, and free electron fraction plotted as functions of distance from the center of the minihalo at the time when the density reaches  $n_{\text{res}}$ , at a redshift of  $z \sim 19$ . The temperature of the gas has dropped to below  $10^3$  K, well below the virial temperature of the minihalo, owing to molecular cooling. Owing to the high electron fraction that persists in this relic H II region, the molecule fraction in this gas is higher than in the case of un-ionized primordial gas collapsing into a minihalo. Indeed, as can be seen in Figure 3, the HD fraction is roughly an order of magnitude higher at these densities than in the case of un-ionized gas collapsing into a minihalo, which may allow for the efficient cooling of the gas to temperatures  $T \gtrsim T_{\text{CMB}}$  and so perhaps for the formation of metal-free stars with masses of the order of  $10 M_{\odot}$ .

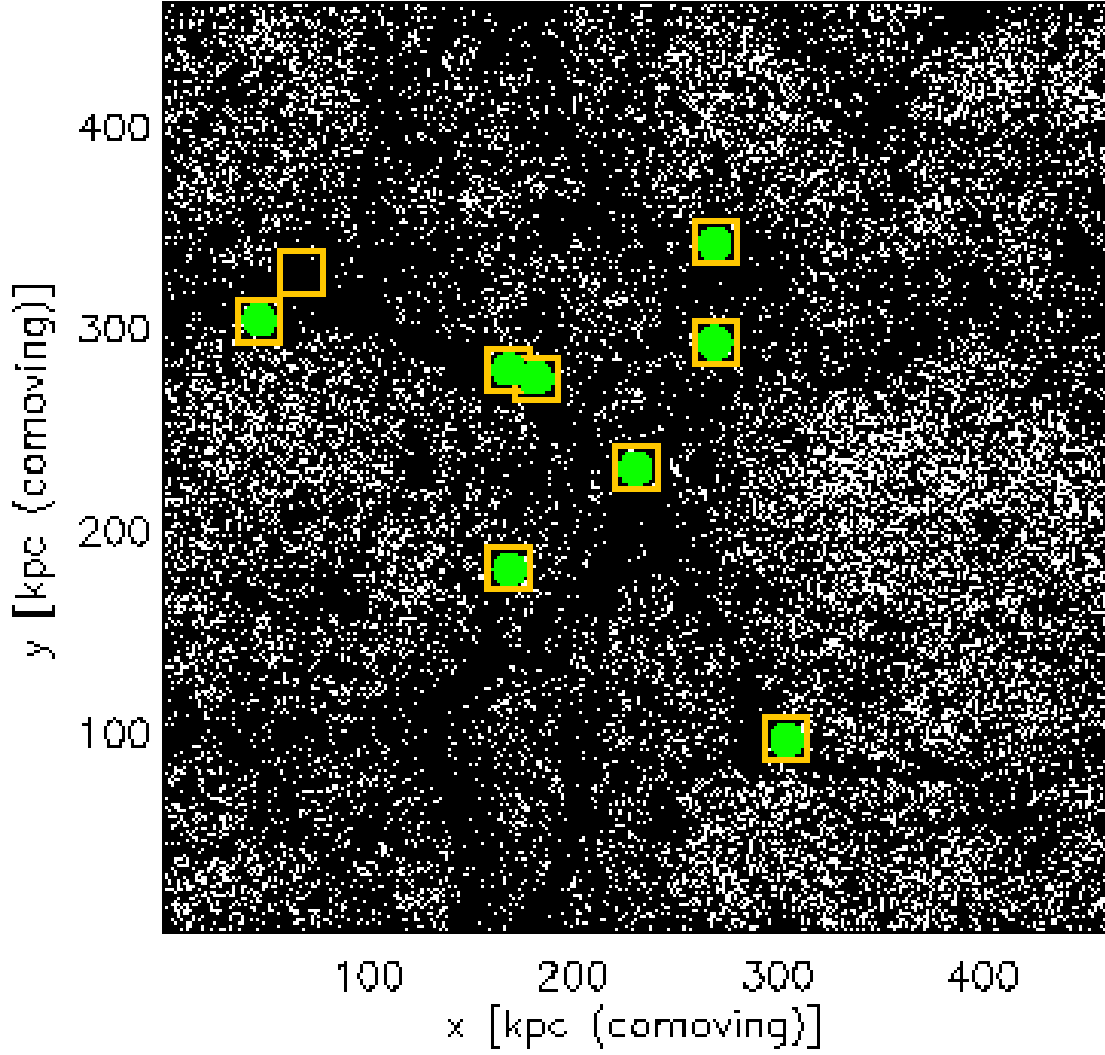


Fig. 7.— The sites of star formation with and without radiative feedback, at redshift  $z \sim 18$ . The black dots show the density field in our simulation box, in projection. The orange squares show the locations of minihalos in which Pop III star formation could take place, in our simulation without radiative feedback. The green dots show the sites where star formation takes place in our simulation including radiative feedback.